

Observation of the Leptonic Decay $D^+ \rightarrow \tau^+ \nu_\tau$

M. Ablikim¹, M. N. Achasov^{10,d}, P. Adlarson⁵⁹, S. Ahmed¹⁵, M. Albrecht⁴, M. Alekseev^{58A,58C}, A. Amoroso^{58A,58C}, F. F. An¹, Q. An^{55,43}, Y. Bai⁴², O. Bakina²⁷, R. Baldini Ferroli^{23A}, I. Balossino^{24A}, Y. Ban³⁵, K. Begzsuren²⁵, J. V. Bennett⁵, N. Berger²⁶, M. Bertani^{23A}, D. Bettoni^{24A}, F. Bianchi^{58A,58C}, J. Biernat⁵⁹, J. Bloms⁵², I. Boyko²⁷, R. A. Briere⁵, H. Cai⁶⁰, X. Cai^{1,43}, A. Calcaterra^{23A}, G. F. Cao^{1,47}, N. Cao^{1,47}, S. A. Cetin^{46B}, J. Chai^{58C}, J. F. Chang^{1,43}, W. L. Chang^{1,47}, G. Chelkov^{27,b,c}, D. Y. Chen⁶, G. Chen¹, H. S. Chen^{1,47}, J. C. Chen¹, M. L. Chen^{1,43}, S. J. Chen³³, Y. B. Chen^{1,43}, W. Cheng^{58C}, G. Cibinetto^{24A}, F. Cossio^{58C}, X. F. Cui³⁴, H. L. Dai^{1,43}, J. P. Dai^{38,h}, X. C. Dai^{1,47}, A. Dbeyssi¹⁵, D. Dedovich²⁷, Z. Y. Deng¹, A. Denig²⁶, I. Denysenko²⁷, M. Destefanis^{58A,58C}, F. De Mori^{58A,58C}, Y. Ding³¹, C. Dong³⁴, J. Dong^{1,43}, L. Y. Dong^{1,47}, M. Y. Dong^{1,43,47}, Z. L. Dou³³, S. X. Du⁶³, J. Z. Fan⁴⁵, J. Fang^{1,43}, S. S. Fang^{1,47}, Y. Fang¹, R. Farinelli^{24A,24B}, L. Fava^{58B,58C}, F. Feldbauer⁴, G. Felici^{23A}, C. Q. Feng^{55,43}, M. Fritsch⁴, C. D. Fu¹, Y. Fu¹, Q. Gao¹, X. L. Gao^{55,43}, Y. Gao⁴⁵, Y. G. Gao⁶, Z. Gao^{55,43}, B. Garillon²⁶, I. Garzia^{24A}, E. M. Gersabeck⁵⁰, A. Gilman⁵¹, K. Goetzen¹¹, L. Gong³⁴, W. X. Gong^{1,43}, W. Gradl²⁶, M. Greco^{58A,58C}, L. M. Gu³³, E. H. Gu^{1,43}, S. Gu², Y. T. Gu¹³, A. Q. Guo²², L. B. Guo³², R. P. Guo³⁶, Y. P. Guo²⁶, A. Guskov²⁷, S. Han⁶⁰, X. Q. Hao¹⁶, F. A. Harris⁴⁸, K. L. He^{1,47}, F. H. Heinsius⁴, T. Held⁴, Y. K. Heng^{1,43,47}, M. Himmelreich^{11,g}, Y. R. Hou⁴⁷, Z. L. Hou¹, H. M. Hu^{1,47}, J. F. Hu^{38,h}, T. Hu^{1,43,47}, Y. Hu¹, G. S. Huang^{55,43}, J. S. Huang¹⁶, X. T. Huang³⁷, X. Z. Huang³³, N. Huesken⁵², T. Hussain⁵⁷, W. Ikegami Andersson⁵⁹, W. Imoehl²², M. Irshad^{55,43}, Q. Ji¹, Q. P. Ji¹⁶, X. B. Ji^{1,47}, X. L. Ji^{1,43}, H. L. Jiang³⁷, X. S. Jiang^{1,43,47}, X. Y. Jiang³⁴, J. B. Jiao³⁷, Z. Jiao¹⁸, D. P. Jin^{1,43,47}, S. Jin³³, Y. Jin⁴⁹, T. Johansson⁵⁹, N. Kalantar-Nayestanaki²⁹, X. S. Kang³¹, R. Kappert²⁹, M. Kavatsyuk²⁹, B. C. Ke¹, I. K. Keshk⁴, A. Khokkaz⁵², P. Kiese²⁶, R. Kiuchi¹, R. Kliemt¹¹, L. Koch²⁸, O. B. Kolcu^{46B,f}, B. Kopf⁴, M. Kuemmel⁴, M. Kuessner⁴, A. Kupsc⁵⁹, M. Kurth¹, M. G. Kurth^{1,47}, W. Kühn²⁸, J. S. Lange²⁸, P. Larin¹⁵, L. Lavezzi^{58C}, H. Leithoff²⁶, T. Lenz²⁶, C. Li⁵⁹, Cheng Li^{55,43}, D. M. Li⁶³, F. Li^{1,43}, F. Y. Li³⁵, G. Li¹, H. B. Li^{1,47}, H. J. Li^{9,j}, J. C. Li¹, J. W. Li⁴¹, Ke Li¹, L. K. Li¹, Lei Li³, P. L. Li^{55,43}, P. R. Li³⁰, Q. Y. Li³⁷, W. D. Li^{1,47}, W. G. Li¹, X. H. Li^{55,43}, X. L. Li³⁷, X. N. Li^{1,43}, Z. B. Li⁴⁴, Z. Y. Li⁴⁴, H. Liang^{55,43}, H. Liang^{1,47}, Y. F. Liang⁴⁰, Y. T. Liang²⁸, G. R. Liao¹², L. Z. Liao^{1,47}, J. Libby²¹, C. X. Lin⁴⁴, D. X. Lin¹⁵, Y. J. Lin¹³, B. Liu^{38,h}, B. J. Liu¹, C. X. Liu¹, D. Liu^{55,43}, D. Y. Liu^{38,h}, F. H. Liu³⁹, Fang Liu¹, Feng Liu⁶, H. B. Liu¹³, H. M. Liu^{1,47}, Huanhuan Liu¹, Huihui Liu¹⁷, J. B. Liu^{55,43}, J. Y. Liu^{1,47}, K. Y. Liu³¹, Ke Liu⁶, L. Y. Liu¹³, Q. Liu⁴⁷, S. B. Liu^{55,43}, T. Liu^{1,47}, X. Liu³⁰, X. Y. Liu^{1,47}, Y. B. Liu³⁴, Z. A. Liu^{1,43,47}, Zhigang Liu³⁷, Y. F. Long³⁵, X. C. Lou^{1,43,47}, H. J. Lu¹⁸, J. D. Lu^{1,47}, J. G. Lu^{1,43}, Y. Lu¹, Y. P. Lu^{1,43}, C. L. Luo³², M. X. Luo⁶², P. W. Luo⁴⁴, T. Luo^{9,j}, X. L. Luo^{1,43}, S. Lusso^{58C}, X. R. Lyu⁴⁷, F. C. Ma³¹, H. L. Ma¹, L. L. Ma³⁷, M. M. Ma^{1,47}, Q. M. Ma¹, X. N. Ma³⁴, X. X. Ma^{1,47}, X. Y. Ma^{1,43}, Y. M. Ma³⁷, F. E. Maas¹⁵, M. Maggiora^{58A,58C}, S. Maldaner²⁶, S. Malde⁵³, Q. A. Malik⁵⁷, A. Mangoni^{23B}, Y. J. Mao³⁵, Z. P. Mao¹, S. Marcello^{58A,58C}, Z. X. Meng⁴⁹, J. G. Messchendorp²⁹, G. Mezzadri^{24A}, J. Min^{1,43}, T. J. Min³³, R. E. Mitchell²², X. H. Mo^{1,43,47}, Y. J. Mo⁶, C. Morales Morales¹⁵, N. Yu. Muchnoi^{10,d}, H. Muramatsu⁵¹, A. Mustafa⁴, S. Nakhoul^{11,g}, Y. Nefedov²⁷, F. Nerling^{11,g}, I. B. Nikolaev^{10,d}, Z. Ning^{1,43}, S. Nisar^{8,k}, S. L. Niu^{1,43}, S. L. Olsen⁴⁷, Q. Ouyang^{1,43,47}, S. Pacetti^{23B}, Y. Pan^{55,43}, M. Papenbrock⁵⁹, P. Patteri^{23A}, M. Pelizaeus⁴, H. P. Peng^{55,43}, K. Peters^{11,g}, J. Pettersson⁵⁹, J. L. Ping³², R. G. Ping^{1,47}, A. Pitka⁴, R. Poling⁵¹, V. Prasad^{55,43}, H. R. Qi², M. Qi³³, T. Y. Qi², S. Qian^{1,43}, C. F. Qiao⁴⁷, N. Qin⁶⁰, X. P. Qin¹³, X. S. Qin⁴, Z. H. Qin^{1,43}, J. F. Qiu¹, S. Q. Qu³⁴, K. H. Rashid^{57,i}, K. Ravindran²¹, C. F. Redmer²⁶, M. Richter⁴, A. Rivetti^{58C}, V. Rodin²⁹, M. Rolo^{58C}, G. Rong^{1,47}, Ch. Rosner¹⁵, M. Rump⁵², A. Sarantsev^{27,e}, M. Savrie^{24B}, Y. Schelhaas²⁶, K. Schoenning⁵⁹, W. Shan¹⁹, X. Y. Shan^{55,43}, M. Shao^{55,43}, C. P. Shen², P. X. Shen³⁴, X. Y. Shen^{1,47}, H. Y. Sheng¹, X. Shi^{1,43}, X. D. Shi^{55,43}, J. J. Song³⁷, Q. Q. Song^{55,43}, X. Y. Song¹, S. Sosio^{58A,58C}, C. Sowa⁴, S. Spataro^{58A,58C}, F. F. Sui³⁷, G. X. Sun¹, J. F. Sun¹⁶, L. Sun⁶⁰, S. S. Sun^{1,47}, X. H. Sun¹, Y. J. Sun^{55,43}, Y. K. Sun^{55,43}, Y. Z. Sun¹, Z. J. Sun^{1,43}, Z. T. Sun¹, Y. T. Tan^{55,43}, C. J. Tang⁴⁰, G. Y. Tang¹, X. Tang¹, V. Thoren⁵⁹, B. Tsednee²⁵, I. Uman^{46D}, B. Wang¹, B. L. Wang⁴⁷, C. W. Wang³³, D. Y. Wang³⁵, K. Wang^{1,43}, L. L. Wang¹, L. S. Wang¹, M. Wang³⁷, M. Z. Wang³⁵, Meng Wang^{1,47}, P. L. Wang¹, R. M. Wang⁶¹, W. P. Wang^{55,43}, X. Wang³⁵, X. F. Wang¹, X. L. Wang^{9,j}, Y. Wang^{55,43}, Y. Wang⁴⁴, Y. F. Wang^{1,43,47}, Z. Wang^{1,43}, Z. G. Wang^{1,43}, Z. Y. Wang¹, Zongyuan Wang^{1,47}, T. Weber⁴, D. H. Wei¹², P. Weidenkaff²⁶, H. W. Wen³², S. P. Wen¹, U. Wiedner⁴, G. Wilkinson⁵³, M. Wolke⁵⁹, L. H. Wu¹, L. J. Wu^{1,47}, Z. Wu^{1,43}, L. Xia^{55,43}, Y. Xia²⁰, S. Y. Xiao¹, Y. J. Xiao^{1,47}, Z. J. Xiao³², Y. G. Xie^{1,43}, Y. H. Xie⁶, T. Y. Xing^{1,47}, X. A. Xiong^{1,47}, Q. L. Xiu^{1,43}, G. F. Xu¹, J. J. Xu³³, L. Xu¹, Q. J. Xu¹⁴, W. Xu^{1,47}, X. P. Xu⁴¹, F. Yan⁵⁶, L. Yan^{58A,58C}, W. B. Yan^{55,43}, W. C. Yan², Y. H. Yan²⁰, H. J. Yang^{38,h}, H. X. Yang¹, L. Yang⁶⁰, R. X. Yang^{55,43}, S. L. Yang^{1,47}, Y. H. Yang³³, Y. X. Yang¹², Yifan Yang^{1,47}, Z. Q. Yang²⁰, M. Ye^{1,43}, M. H. Ye⁷, J. H. Yin¹, Z. Y. You⁴⁴, B. X. Yu^{1,43,47}, C. X. Yu³⁴, J. S. Yu²⁰, T. Yu⁵⁶, C. Z. Yuan^{1,47}, X. Q. Yuan³⁵, Y. Yuan¹, A. Yuncu^{46B,a}, A. A. Zafar⁵⁷, Y. Zeng²⁰, B. X. Zhang¹, B. Y. Zhang^{1,43}, C. C. Zhang¹, D. H. Zhang¹, H. H. Zhang⁴⁴, H. Y. Zhang^{1,43}, J. Zhang^{1,47}, J. L. Zhang⁶¹, J. Q. Zhang⁴, J. W. Zhang^{1,43,47}, J. Y. Zhang¹, J. Z. Zhang^{1,47}, K. Zhang⁴⁵, S. F. Zhang³³, T. J. Zhang^{38,h}, X. Y. Zhang³⁷, Y. Zhang^{55,43}, Y. H. Zhang^{1,43}, Y. T. Zhang^{55,43}, Yang Zhang¹, Yao Zhang¹, Yi Zhang^{9,j}, Yu Zhang⁴⁷, Z. H. Zhang⁶, Z. P. Zhang⁵⁵, Z. Y. Zhang⁶⁰, G. Zhao¹, J. W. Zhao^{1,43}, J. Y. Zhao^{1,47}, J. Z. Zhao^{1,43}, Lei Zhao^{55,43}, Ling Zhao¹, M. G. Zhao³⁴, Q. Zhao¹, S. J. Zhao⁶³, T. C. Zhao¹, Y. B. Zhao^{1,43}, Z. G. Zhao^{55,43}, A. Zhemchugov^{27,b}, B. Zheng⁵⁶, J. P. Zheng^{1,43}, Y. Zheng³⁵, Y. H. Zheng⁴⁷, B. Zhong³², L. Zhou^{1,43}, L. P. Zhou^{1,47}, Q. Zhou^{1,47}, X. Zhou⁶⁰, X. K. Zhou⁵⁴, X. R. Zhou^{55,43}, Xiaoyu Zhou²⁰, Xu Zhou²⁰, A. N. Zhu^{1,47}, J. Zhu³⁴, J. Zhu⁴⁴, K. Zhu¹, K. J. Zhu^{1,43,47}, S. H. Zhu⁵⁴, W. J. Zhu³⁴, X. L. Zhu⁴⁵, Y. C. Zhu^{55,43}, Y. S. Zhu^{1,47}, Z. A. Zhu^{1,47}, J. Zhuang^{1,43}, B. S. Zou¹, J. H. Zou¹

(BESIII Collaboration)

- ¹ *Institute of High Energy Physics, Beijing 100049, People's Republic of China*
- ² *Beihang University, Beijing 100191, People's Republic of China*
- ³ *Beijing Institute of Petrochemical Technology, Beijing 102617, People's Republic of China*
- ⁴ *Bochum Ruhr-University, D-44780 Bochum, Germany*
- ⁵ *Carnegie Mellon University, Pittsburgh, Pennsylvania 15213, USA*
- ⁶ *Central China Normal University, Wuhan 430079, People's Republic of China*
- ⁷ *China Center of Advanced Science and Technology, Beijing 100190, People's Republic of China*
- ⁸ *COMSATS University Islamabad, Lahore Campus, Defence Road, Off Raiwind Road, 54000 Lahore, Pakistan*
- ⁹ *Fudan University, Shanghai 200443, People's Republic of China*
- ¹⁰ *G.I. Budker Institute of Nuclear Physics SB RAS (BINP), Novosibirsk 630090, Russia*
- ¹¹ *GSI Helmholtzcentre for Heavy Ion Research GmbH, D-64291 Darmstadt, Germany*
- ¹² *Guangxi Normal University, Guilin 541004, People's Republic of China*
- ¹³ *Guangxi University, Nanning 530004, People's Republic of China*
- ¹⁴ *Hangzhou Normal University, Hangzhou 310036, People's Republic of China*
- ¹⁵ *Helmholtz Institute Mainz, Johann-Joachim-Becher-Weg 45, D-55099 Mainz, Germany*
- ¹⁶ *Henan Normal University, Xinxiang 453007, People's Republic of China*
- ¹⁷ *Henan University of Science and Technology, Luoyang 471003, People's Republic of China*
- ¹⁸ *Huangshan College, Huangshan 245000, People's Republic of China*
- ¹⁹ *Hunan Normal University, Changsha 410081, People's Republic of China*
- ²⁰ *Hunan University, Changsha 410082, People's Republic of China*
- ²¹ *Indian Institute of Technology Madras, Chennai 600036, India*
- ²² *Indiana University, Bloomington, Indiana 47405, USA*
- ²³ *(A)INFN Laboratori Nazionali di Frascati, I-00044, Frascati, Italy; (B)INFN and University of Perugia, I-06100, Perugia, Italy*
- ²⁴ *(A)INFN Sezione di Ferrara, I-44122, Ferrara, Italy; (B)University of Ferrara, I-44122, Ferrara, Italy*
- ²⁵ *Institute of Physics and Technology, Peace Ave. 54B, Ulaanbaatar 13330, Mongolia*
- ²⁶ *Johannes Gutenberg University of Mainz, Johann-Joachim-Becher-Weg 45, D-55099 Mainz, Germany*
- ²⁷ *Joint Institute for Nuclear Research, 141980 Dubna, Moscow region, Russia*
- ²⁸ *Justus-Liebig-Universitaet Giessen, II. Physikalisches Institut, Heinrich-Buff-Ring 16, D-35392 Giessen, Germany*
- ²⁹ *KVI-CART, University of Groningen, NL-9747 AA Groningen, The Netherlands*
- ³⁰ *Lanzhou University, Lanzhou 730000, People's Republic of China*
- ³¹ *Liaoning University, Shenyang 110036, People's Republic of China*
- ³² *Nanjing Normal University, Nanjing 210023, People's Republic of China*
- ³³ *Nanjing University, Nanjing 210093, People's Republic of China*
- ³⁴ *Nankai University, Tianjin 300071, People's Republic of China*
- ³⁵ *Peking University, Beijing 100871, People's Republic of China*
- ³⁶ *Shandong Normal University, Jinan 250014, People's Republic of China*
- ³⁷ *Shandong University, Jinan 250100, People's Republic of China*
- ³⁸ *Shanghai Jiao Tong University, Shanghai 200240, People's Republic of China*
- ³⁹ *Shanxi University, Taiyuan 030006, People's Republic of China*
- ⁴⁰ *Sichuan University, Chengdu 610064, People's Republic of China*
- ⁴¹ *Soochow University, Suzhou 215006, People's Republic of China*
- ⁴² *Southeast University, Nanjing 211100, People's Republic of China*
- ⁴³ *State Key Laboratory of Particle Detection and Electronics, Beijing 100049, Hefei 230026, People's Republic of China*
- ⁴⁴ *Sun Yat-Sen University, Guangzhou 510275, People's Republic of China*
- ⁴⁵ *Tsinghua University, Beijing 100084, People's Republic of China*
- ⁴⁶ *(A)Ankara University, 06100 Tandogan, Ankara, Turkey; (B)Istanbul Bilgi University, 34060 Eyup, Istanbul, Turkey; (C)Uludag University, 16059 Bursa, Turkey; (D)Near East University, Nicosia, North Cyprus, Mersin 10, Turkey*
- ⁴⁷ *University of Chinese Academy of Sciences, Beijing 100049, People's Republic of China*
- ⁴⁸ *University of Hawaii, Honolulu, Hawaii 96822, USA*
- ⁴⁹ *University of Jinan, Jinan 250022, People's Republic of China*
- ⁵⁰ *University of Manchester, Oxford Road, Manchester, M13 9PL, United Kingdom*
- ⁵¹ *University of Minnesota, Minneapolis, Minnesota 55455, USA*
- ⁵² *University of Muenster, Wilhelm-Klemm-Str. 9, 48149 Muenster, Germany*
- ⁵³ *University of Oxford, Keble Rd, Oxford, OX13RH United Kingdom*
- ⁵⁴ *University of Science and Technology Liaoning, Anshan 114051, People's Republic of China*
- ⁵⁵ *University of Science and Technology of China, Hefei 230026, People's Republic of China*
- ⁵⁶ *University of South China, Hengyang 421001, People's Republic of China*
- ⁵⁷ *University of the Punjab, Lahore-54590, Pakistan*
- ⁵⁸ *(A)University of Turin, I-10125, Turin, Italy; (B)University of Eastern Piedmont, I-15121, Alessandria, Italy; (C)INFN, I-10125, Turin, Italy*
- ⁵⁹ *Uppsala University, Box 516, SE-75120 Uppsala, Sweden*

⁶⁰ Wuhan University, Wuhan 430072, People's Republic of China

⁶¹ Xinyang Normal University, Xinyang 464000, People's Republic of China

⁶² Zhejiang University, Hangzhou 310027, People's Republic of China

⁶³ Zhengzhou University, Zhengzhou 450001, People's Republic of China

^a Also at Bogazici University, 34342 Istanbul, Turkey

^b Also at the Moscow Institute of Physics and Technology, Moscow 141700, Russia

^c Also at the Functional Electronics Laboratory, Tomsk State University, Tomsk, 634050, Russia

^d Also at the Novosibirsk State University, Novosibirsk, 630090, Russia

^e Also at the NRC "Kurchatov Institute", PNPI, 188300 Gatchina, Russia

^f Also at Istanbul Arel University, 34295 Istanbul, Turkey

^g Also at Goethe University Frankfurt, 60323 Frankfurt am Main, Germany

^h Also at Key Laboratory for Particle Physics, Astrophysics and Cosmology, Ministry of Education; Shanghai Key Laboratory for Particle Physics and Cosmology; Institute of Nuclear and Particle Physics, Shanghai 200240, People's Republic of China

ⁱ Also at Government College Women University, Sialkot-51310. Punjab, Pakistan.

^j Also at Key Laboratory of Nuclear Physics and Ion-beam Application (MOE) and Institute of Modern Physics, Fudan University, Shanghai 200443, People's Republic of China

^k Also at Harvard University, Department of Physics, Cambridge, Massachusetts 02138, USA

We report the first observation of $D^+ \rightarrow \tau^+ \nu_\tau$ with a significance of 5.1σ . We measure $\mathcal{B}(D^+ \rightarrow \tau^+ \nu_\tau) = (1.20 \pm 0.24_{\text{stat.}} \pm 0.12_{\text{syst.}}) \times 10^{-3}$. Taking the world average $\mathcal{B}(D^+ \rightarrow \mu^+ \nu_\mu) = (3.74 \pm 0.17) \times 10^{-4}$, we obtain $R_{\tau/\mu} = \Gamma(D^+ \rightarrow \tau^+ \nu_\tau) / \Gamma(D^+ \rightarrow \mu^+ \nu_\mu) = 3.21 \pm 0.64_{\text{stat.}} \pm 0.43_{\text{syst.}}$, which is consistent with the standard model expectation of lepton flavor universality. Using external inputs, our results give values for the D^+ decay constant f_{D^+} and the Cabibbo-Kobayashi-Maskawa matrix element $|V_{cd}|$ that are consistent with, but less precise than, other determinations.

In the purely leptonic decay of the charmed meson D^+ , the c and \bar{d} quarks annihilate into a pair of charged and neutral leptons via a virtual W boson. (Unless otherwise noted, charge conjugate modes are implied throughout this Letter.) To the lowest order, the decay rate for $D^+ \rightarrow \ell^+ \nu_\ell$ is given in a very simple form:

$$\Gamma(D^+ \rightarrow \ell^+ \nu_\ell) = \frac{G_F^2}{8\pi} f_{D^+}^2 |V_{cd}|^2 m_\ell^2 M_{D^+} \left(1 - \frac{m_\ell^2}{M_{D^+}^2}\right)^2, \quad (1)$$

where the D^+ mass M_{D^+} , the masses of the charged leptons m_ℓ ($\ell = e^+, \mu^+, \text{ or } \tau^+$), and the Fermi coupling constant G_F are known to great precision [1]. Because of this, measuring $\mathcal{B}(D^+ \rightarrow \ell^+ \nu_\ell)$ ($\mathcal{B}_{\ell\nu}$) allows determination of the product $f_{D^+}^2 |V_{cd}|^2$ of the D^+ decay constant and the square of the $c \rightarrow d$ Cabibbo-Kobayashi-Maskawa (CKM) matrix element. One can then extract $|V_{cd}|$ by using the predicted value of f_{D^+} , e.g., from lattice quantum chromodynamics (LQCD), or obtain f_{D^+} by using the experimentally measured $|V_{cd}|$ to test the LQCD prediction. Such studies have been done using the muonic mode $D^+ \rightarrow \mu^+ \nu_\mu$ ([2],[3]), which is a simple two-body decay with a clear experimental signature. The energetic track produced in this decay can be reconstructed very efficiently with minimal systematic uncertainty.

Experimental information about $D^+ \rightarrow \tau^+ \nu_\tau$ is more sparse, with only an upper limit of 1.2×10^{-3} on $\mathcal{B}_{\tau\nu}$ at a 90% confidence level (C.L.) [1] that was set by the CLEO Collaboration [3]. Measuring $\mathcal{B}_{\tau\nu}$ is an important check of the standard model, which predicts the ratio of the $\tau^+ \nu_\tau$ and $\mu^+ \nu_\mu$ decay rates. Applying Eq. (1) to both

$D^+ \rightarrow \mu^+ \nu_\mu$ and $D^+ \rightarrow \tau^+ \nu_\tau$, we find

$$R_{\tau/\mu} = \frac{\Gamma(D^+ \rightarrow \tau^+ \nu_\tau)}{\Gamma(D^+ \rightarrow \mu^+ \nu_\mu)} = \frac{m_\tau^2 (1 - \frac{m_\tau^2}{M_{D^+}^2})^2}{m_\mu^2 (1 - \frac{m_\mu^2}{M_{D^+}^2})^2} = 2.67, \quad (2)$$

which provides a clean test of the standard model expectation of lepton flavor universality. Deviation from the expected value of $R_{\tau/\mu}$ could signify contributions of a charged intermediate boson that couples to the leptons differently, e.g., through a leptoquark [4]. The fact that $\mathcal{B}_{\tau\nu}$ has not been measured previously, together with the recent hints of possible violation of lepton universality in B decays [5], establishes that $R_{\tau/\mu}$ is an important quantity to determine experimentally. We note, however, that in some supersymmetric models, such as the two-Higgs-doublet model [6], the charged Higgs couples to the lepton mass leading to a mass dependence identical to that from the W boson process, including its helicity suppression. Thus, Eq. (1) is modified by a factor that does not depend on the lepton masses, leaving $R_{\tau/\mu}$ unchanged.

From the standard model prediction $R_{\tau/\mu} = 2.67$ and $\mathcal{B}_{\mu\nu} = (3.74 \pm 0.17) \times 10^{-4}$ [1], one expects $\mathcal{B}_{\tau\nu} = (1.01 \pm 0.05) \times 10^{-3}$, which is very close to CLEO's upper limit based on 818 pb^{-1} of e^+e^- annihilation data. In this Letter, we report the first observation of $D^+ \rightarrow \tau^+ \nu_\tau$ and the measurement of its branching fraction with an e^+e^- annihilation sample produced at the Beijing Electron Positron Collider (BEPCII) [7] near the nominal mass of the $\psi(3770)$ resonance, $\sqrt{s} = 3.773$ GeV, with an integrated luminosity of 2931.8 pb^{-1} [8] collected with the BESIII detector.

BESIII is a cylindrical detector with a solid angle coverage of 93% of 4π . The detector consists of a Helium-gas-based main drift chamber (MDC), a plastic scintillator time-of-flight system, a CsI(Tl) electromagnetic calorimeter (EMC), a superconducting solenoid providing a 1.0 T magnetic field, and muon counters. The charged particle momentum resolution is 0.5% at a transverse momentum of 1 GeV/c. The photon energy resolution at 1 GeV is 2.5% in the central barrel region and 5.0% in the end cap region. More details about the design and performance of BESIII are given in Ref. [9].

Detection efficiencies and background processes are determined with a Monte Carlo (MC) simulation sample with an equivalent luminosity roughly 10 times larger than the data set. It consists of events from $e^+e^- \rightarrow \psi(3770) \rightarrow D\bar{D}$, $e^+e^- \rightarrow q\bar{q}$ ($q = u, d, s$), $e^+e^- \rightarrow \gamma J/\psi$, $e^+e^- \rightarrow \gamma\psi(3686)$, and $e^+e^- \rightarrow \tau^+\tau^-$. The effects of initial- and final-state radiation are simulated by the KKMC generator [10] and the PHOTOS package [11], respectively. The generated four-momenta are propagated into EVTGEN [12], which simulates decays using known rates [13] and correct angular distributions. We generate charmonium decays not accounted for by exclusive measurements with LUNDCHARM [14]. Finally, the detector response is simulated with GEANT4 [15].

We measure $\mathcal{B}_{\tau\nu}$ by reconstructing τ^+ via $\tau^+ \rightarrow \pi^+\bar{\nu}_\tau$, which has the feature of only a single charged track from the D^+ decay. Because pions and muons are charged particles with similar masses, the BESIII selection of pion tracks based on specific-ionization and time-of-flight measurements also accepts muon tracks with comparable efficiency ($> 90\%$), allowing simultaneous measurement of $\mathcal{B}_{\tau\nu}$ and $\mathcal{B}_{\mu\nu}$. For this analysis our main result is obtained by fixing $\mathcal{B}_{\mu\nu}$ to the world average of $(3.74 \pm 0.17) \times 10^{-4}$ [1] to maximize our statistical sensitivity for measuring $\mathcal{B}_{\tau\nu}$. We also perform a cross-check of our result by measuring $\mathcal{B}_{\mu\nu}$ and $\mathcal{B}_{\tau\nu}$ simultaneously.

This analysis employs a double-tag technique, pioneered by the Mark III Collaboration [16]. We obtain the branching fraction by reconstructing $D^+ \rightarrow \tau^+(\rightarrow \pi^+\bar{\nu}_\tau)\nu_\tau$ in events with D^- decays reconstructed in one of the six tag modes listed in Table I:

$$\mathcal{B}_{\tau\nu} = \frac{N_{\tau\nu}}{\sum_i N_{\text{tag}}^i (\epsilon_{\tau\nu}^i / \epsilon_{\text{tag}}^i)}. \quad (3)$$

In Eq. (3) $N_{\tau\nu}$ is the number of events with any D^- tag and a $D^+ \rightarrow \tau^+(\rightarrow \pi^+\bar{\nu}_\tau)\nu_\tau$ candidate, $\epsilon_{\tau\nu}^i$ is the signal selection efficiency including $\mathcal{B}(\tau^+ \rightarrow \pi^+\bar{\nu}_\tau)$ for an event with a D^- in the i th tag mode, and N_{tag}^i and ϵ_{tag}^i are the number of tag and reconstruction efficiency for D^- tags in mode i .

In selecting tags our criteria for the final-state particles are identical to those in Ref. [17]. In each event, we allow only one D candidate for a given tag mode separately for D^+ and D^- , following the method of Ref. [18]. For each tag mode, we extract N_{tag}^i from distributions

of beam-constrained mass $M_{\text{BC}}c^2 = \sqrt{E_{\text{beam}}^2 - |\vec{p}_{\text{tag}}|^2}$, where \vec{p}_{tag} is the three-momentum of the tag D^- candidate and E_{beam} is the beam energy in the center-of-mass system of the $\psi(3770)$. We fit to these M_{BC} distributions with MC-based signal shapes that are convolved with a Gaussian to accommodate resolution differences between simulation and data. The background shape is parametrized with an ARGUS function [19]. Figure 1 shows the fits to M_{BC} distributions. To select the tag, we require that $1863 < M_{\text{BC}} < 1877 \text{ MeV}/c^2$ [20]. Table I shows N_{tag}^i , ϵ_{tag}^i , and $\epsilon_{\tau\nu}^i$ for all tag modes.

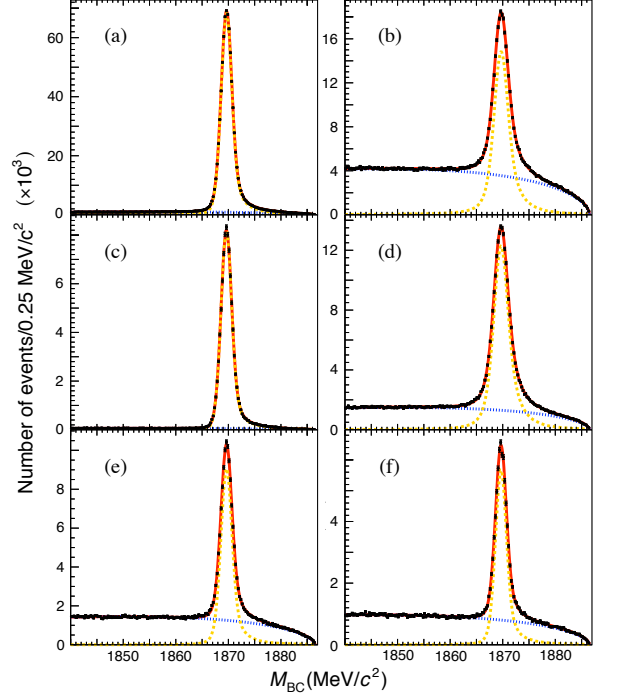


FIG. 1. Fits to M_{BC} distributions of single-tag D^- candidates for the full data sample for tag modes $D^- \rightarrow$ (a) $K^+\pi^-\pi^-$, (b) $K^+\pi^-\pi^-\pi^0$, (c) $K_S^0\pi^-$, (d) $K_S^0\pi^-\pi^0$, (e) $K_S^0\pi^-\pi^-\pi^+$, and (f) $K^+K^-\pi^-$. Red lines are the overall fits, while the yellow-dashed (blue-dotted) lines are the fitted signals (backgrounds).

TABLE I. Single-tag efficiencies (ϵ_{tag}^i) and yields (N_{tag}^i), and signal selection efficiencies ($\epsilon_{\tau\nu}^i$). Efficiencies are corrected for $\mathcal{B}(K_S^0 \rightarrow \pi^+\pi^-)$ and $\mathcal{B}(\pi^0 \rightarrow \gamma\gamma)$.

Tag modes, i	$N_{\text{tag}}^i (\times 10^3)$	$\epsilon_{\text{tag}}^i (\%)$	$\epsilon_{\tau\nu}^i (\%)$
$K^+\pi^-\pi^-$	797.6 ± 1.0	51.06 ± 0.03	3.6 ± 0.1
$K^+\pi^-\pi^-\pi^0$	245.1 ± 0.7	25.18 ± 0.03	2.1 ± 0.1
$K_S^0\pi^-$	92.6 ± 0.3	50.66 ± 0.07	4.0 ± 0.1
$K_S^0\pi^-\pi^0$	206.3 ± 0.6	26.09 ± 0.03	2.1 ± 0.1
$K_S^0\pi^-\pi^-\pi^+$	110.2 ± 0.4	26.75 ± 0.04	2.2 ± 0.1
$K^+K^-\pi^-$	68.1 ± 0.3	40.38 ± 0.08	3.1 ± 0.1

Once we select the tag, we require that there be only one additional charged track and that it have charge opposite to that of the tag. It must originate within 1 cm (10 cm) from the beam interaction point in the plane transverse to (along) the beam direction, be within the fiducial region for reliable track reconstruction ($|\cos\theta| < 0.93$, where θ is the polar angle with respect to the direction of the positron beam), and match a shower in the EMC. Furthermore, to distinguish between π -like and μ -like tracks, we rely on the minimum-ionizing character of the μ track, which has a mean energy deposit of $E_{\text{EMC}} \simeq 200$ MeV, as was done in Refs. [2, 3]. Thus we partition the selected events into two samples, one with μ -like tracks ($E_{\text{EMC}} \leq 300$ MeV) and the other with π -like tracks ($E_{\text{EMC}} > 300$ MeV). The first portion includes 99% of the muon tracks from $D^+ \rightarrow \mu^+ \nu_\mu$, while the second has 44% of the pion tracks from $D^+ \rightarrow \tau^+ \nu_\tau$, $\tau^+ \rightarrow \pi^+ \bar{\nu}_\tau$.

To suppress backgrounds further, we apply four additional requirements, which are optimized based on MC calculations. (1) $E_{\text{EMC}}/|\vec{p}c| < 0.95$ for the π -like sample, where \vec{p} is the signal track momentum measured by the MDC. As this variable sharply peaks around 1 for an electron, this requirement suppresses events from semileptonic decays like $D^+ \rightarrow K_L^0 e^+ \nu_e$. (2) $E_{\text{max}} < 300$ MeV for both samples, where E_{max} is the maximum energy of all EMC showers that are not assigned to any charged track or neutral EMC shower in the reconstruction of both D^+ and D^- . This suppresses events with extra particles, including misreconstructed neutral pions. (3) $|\cos\theta_{\text{missing}}| < 0.95(0.75)$ for the μ (π)-like sample, where θ_{missing} is the polar angle of the missing momentum $\vec{p}_{\text{missing}} = -\vec{p}_{D^-} - \vec{p}_{\mu(\pi)}$, $\vec{p}_{D^-} = \hat{p}_{D^-} \sqrt{(E_{\text{beam}}/c)^2 - (M_{D^+c})^2}$, and \hat{p}_{D^-} is the unit momentum vector of the D^- . This ensures that \vec{p}_{missing} points to an active region of the detector. (4) $\alpha > 25^\circ(45^\circ)$ for the μ (π)-like sample, where α is the opening angle between \vec{p}_{missing} and the direction of the most energetic unassigned shower. A shower from an asymmetric decay of π^0 or from K_L^0 tends to deposit energy in the EMC in the \vec{p}_{missing} direction. The minimum required energy of the unassigned shower is 25 MeV for $|\cos\theta| < 0.8$ and 50 MeV for $0.86 < |\cos\theta| < 0.93$.

Signals are extracted from the distributions of missing mass-squared $M_{\text{miss}}^2 = E_{\text{missing}}^2 - |\vec{p}_{\text{missing}}c|^2$, where $E_{\text{missing}} = E_{\text{beam}} - E_{\mu(\pi)}$. Events from $D^+ \rightarrow \mu^+ \nu_\mu$ peak around $M_{\text{miss}}^2 = 0$, and the ones from $D^+ \rightarrow \tau^+ \nu_\tau$, where $\tau^+ \rightarrow \pi^+ \bar{\nu}_\tau$, also tend to populate near $M_{\text{miss}}^2 = 0$ because $m_\tau \simeq M_D$.

We expect peaking backgrounds from $D^+ \rightarrow \pi^0 \pi^+$ and $D^+ \rightarrow K_L^0 \pi^+$. The first is relatively small, but is close to $M_{\text{miss}}^2 = 0$. The latter peaks away from $M_{\text{miss}}^2 = 0$ at $m_{K^0}^2$, but is a concern because of an expected rate of 40 times the expected signal.

We use data-based control samples to construct the

probability density functions (PDFs) to represent these two peaking backgrounds. The black points in Fig. 2 show M_{miss}^2 distributions from exclusively reconstructed $D^+ \rightarrow \pi^0(\rightarrow \gamma\gamma)\pi^+$ (left column) and $D^+ \rightarrow K_S^0(\rightarrow \pi^+\pi^-)\pi^+$ (right column) events in which we treat the K_S^0 and the π^0 as missing particles, respectively. The red-shaded histograms are from true $D^+ \rightarrow \pi^0 \pi^+$ and $D^+ \rightarrow K_L^0 \pi^+$ MC events after applying all signal selection criteria, scaled to the same sizes as the data. Agreement between the shapes of the expected distributions and our control samples is excellent. We generate the corresponding PDFs by smoothing the distributions of the data points by the kernel estimation method [21]. Additional peaking backgrounds from $D^+ \rightarrow \eta(\rightarrow \gamma\gamma)\pi^+$

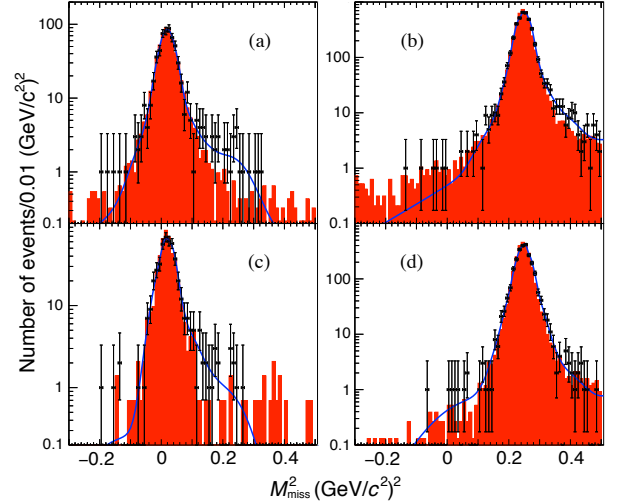


FIG. 2. M_{miss}^2 distributions of $D^+ \rightarrow \pi^0 \pi^+$ (a), (c) and $D^+ \rightarrow K_S^0(\rightarrow \pi^+\pi^-)\pi^+$ (b), (d) events from data (black points) for the μ -like (a), (b) and π -like (c), (d) samples. The blue lines are the PDFs derived from the black points, while the red-shaded histograms are true $D^+ \rightarrow \pi^0 \pi^+$ and $D^+ \rightarrow K_L^0 \pi^+$ MC events with all selection criteria applied.

and $D^+ \rightarrow K_S^0(\rightarrow \pi^0 \pi^0)\pi^+$ are also considered, but both are small and peak away from $M_{\text{miss}}^2 = 0$. For these two small backgrounds, we use the MC events to predict the PDF.

We perform an unbinned simultaneous maximum likelihood fit to the μ - and π -like samples. The signal PDFs are based on MC events, including $D^+ \rightarrow \tau^+ \nu_\tau$ with τ^+ final states other than $\pi^+ \bar{\nu}_\tau$. This contribution is dominated by $\tau^+ \rightarrow \mu^+ \nu_\mu \bar{\nu}_\tau$ and $\pi^+ \pi^0 \bar{\nu}_\tau$ in the μ -like sample, while the π -like sample mostly contains $\tau^+ \rightarrow e^+ \nu_e \bar{\nu}_\tau$ and $\pi^+ \pi^0 \bar{\nu}_\tau$. To take into account the M_{miss}^2 resolution difference between the data and the MC samples, the PDFs of the signal and of the backgrounds are smeared using a Gaussian. The Gaussian mean and width are free parameters of the fit. The remaining background (“smooth background”) comes from other well known D decays, such as semileptonic decays, as well as continuum events. It is represented by the smoothed MC prediction.

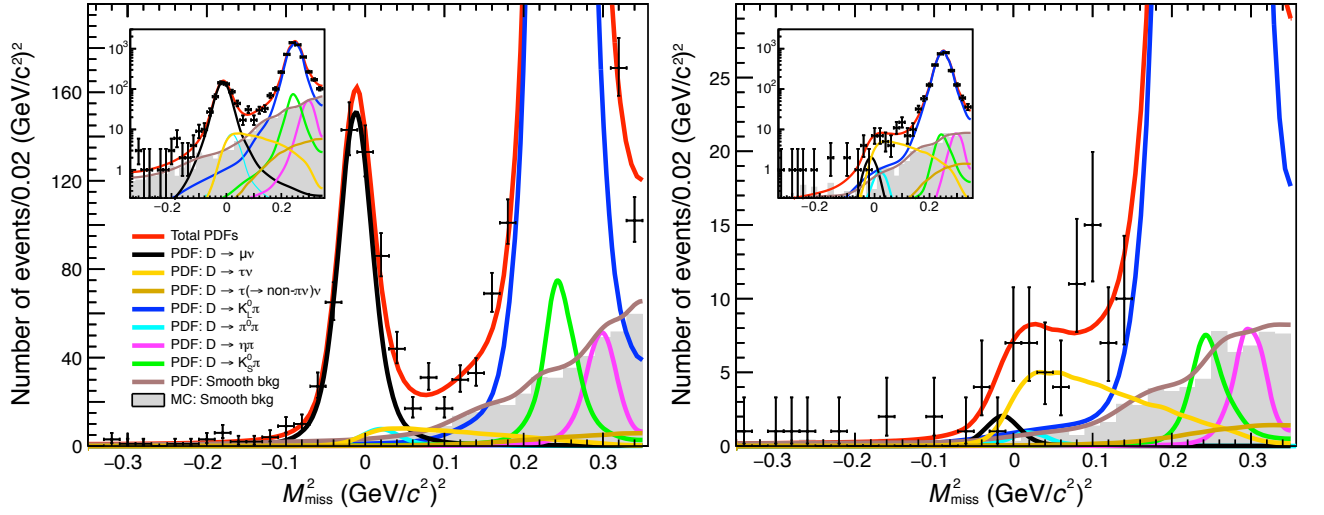


FIG. 3. Fits to M_{miss}^2 distributions of the μ -like (left) and π -like (right) samples. The black points are data and gray-shaded histograms are MC-predicted smooth background components scaled to the data size based on the known production cross sections and measured integrated luminosity. The insets show the same distributions with logarithmic scales.

We fix the sizes of D^+ decays to $\mu^+\nu_\mu$, $\pi^0\pi^+$, $\eta\pi^+$, and $K_S^0\pi^+$ according to Ref. [1], while we leave the normalizations for decays to $\tau^+\nu_\tau$ and $K_L^0\pi^+$, as well as the smooth background as free fit parameters. The ratio of the normalizations of the smooth background between the μ -like and π -like samples is constrained based on the MC prediction. Applying this fitting procedure to the $D\bar{D}$ MC sample, we obtain the signal selection efficiencies $\epsilon_{\tau\nu}^i$ for each tag mode listed in Table I.

Figure 3 shows the simultaneous fit to data, which yields 137 ± 27 signal events. This corresponds to $\mathcal{B}_{\tau\nu} = (1.20 \pm 0.24_{\text{stat.}}) \times 10^{-3}$.

As a cross check, we treat the $D^+ \rightarrow \mu^+\nu_\mu$ component as a free fit parameter and obtain $\mathcal{B}_{\mu\nu} = (3.70 \pm 0.20_{\text{stat.}}) \times 10^{-4}$, along with $\mathcal{B}_{\tau\nu} = (1.21 \pm 0.24_{\text{stat.}}) \times 10^{-3}$. The obtained $\mathcal{B}_{\mu\nu}$ is consistent with both the world average of $(3.74 \pm 0.17) \times 10^{-4}$ [1] and the recent BESIII measurement of $(3.71 \pm 0.19_{\text{stat.}} \pm 0.06_{\text{syst.}}) \times 10^{-4}$ [2]. The agreement with the latter measurement provides independent confirmation, as Ref. [2] uses muon counter information and is based on simulations of the signal efficiency and the background that are different from the current work.

The total systematic uncertainty is dominated by two sources. The first is the uncertainty on $\mathcal{B}_{\mu\nu}$, which is fixed to the value from Ref. [1]. The second is the uncertainty due to the assumed shapes of the smooth background. For this we vary the shape by changing the $e^+e^- \rightarrow \psi(3770) \rightarrow D\bar{D}$ and $e^+e^- \rightarrow q\bar{q}$ cross sections from the defaults in our MC calculations. We also consider two different values of the smoothing parameter ρ in the Gaussian kernel estimation method [21], $\rho = 1$ (the author's suggestion) and $\rho = 2$. The dependence on the choice of 300 MeV for the boundary between π - and

μ -like samples, which potentially changes the shapes of the smooth backgrounds, is also assessed by varying it by ± 50 MeV.

Other sources of systematic uncertainty are also considered. The uncertainty in the signal track reconstruction efficiency has been obtained from previous BESIII studies of double-tagged $D\bar{D}$ events. The uncertainty in $\mathcal{B}(\tau^+ \rightarrow \pi^+\bar{\nu}_\tau)$ is from Ref. [1]. Statistical uncertainties in the tag counts in data and MC calculations are taken directly from the respective samples. Variations in the fit ranges, selection windows, binning, and signal and background parametrizations are used to probe uncertainties in the tag-side fits. We estimate uncertainties due to the $E_{\text{EMC}}/|\vec{p}_c|$ and E_{max} criteria with double-tagged events including $D^+ \rightarrow K_S^0\pi^+$. Uncertainties from the cuts on $|\cos\theta_{\text{missing}}|$ and α are estimated with fully reconstructed $D^0 \rightarrow K^-e^+\nu_e$ events. Possible mismodeling of efficiencies due to multiplicity differences among D decay modes is estimated based on a study of tracking and particle identification efficiencies in different event environments. The uncertainty due to the normalization of the peaking backgrounds, and the ratio of smooth background sizes between μ - and π -like samples in the M_{miss}^2 fit are estimated by studies of the $D^+ \rightarrow K_S^0\pi^+$ control sample and by varying parametrizations and branching fractions, respectively. The $D^+ \rightarrow \tau^+\nu_\tau$ signal-shape dependence is estimated by altering the mixture of τ^+ decay modes. Table II summarizes the systematic uncertainty estimate.

Using the 2.93 fb^{-1} data sample taken at $\sqrt{s} = 3.773 \text{ GeV}$, we measure $\mathcal{B}_{\tau\nu} = (1.20 \pm 0.24_{\text{stat.}} \pm 0.12_{\text{syst.}}) \times 10^{-3}$ using $\mathcal{B}_{\mu\nu} = (3.74 \pm 0.17) \times 10^{-4}$. The signal significance including the systematic uncertainty is 5.1σ , calculated via $\sqrt{-2 \times \ln \mathcal{L}_{\text{null}}/\mathcal{L}}$, where $\mathcal{L}_{\text{null}}$ and \mathcal{L} are likelihood values without and with $D^+ \rightarrow \tau^+\nu_\tau$,

TABLE II. Summary of relative systematic uncertainties in units of 10^{-2} .

Source	$\Delta\mathcal{B}_{\tau\nu}$
$\Delta\mathcal{B}(D^+ \rightarrow \mu^+\nu_\mu)$	6.9
Shape of smooth background	4.2
π^+ tracking	1.0
$\Delta\mathcal{B}(\tau^+ \rightarrow \pi^+\bar{\nu}_\tau)$	0.5
Stat. uncertainties from tag side and MC calculations	2.2
Fitting scheme on tag side	0.5
Requirement on $E_{\text{EMC}}/ \vec{p}c $	2.5
Requirement on E_{max}	2.2
Requirements on $ \cos\theta_{\text{missing}} $ and α	2.1
Tag bias	0.1
Normalizations of small peaking backgrounds	1.9
Relative size of smooth background components	2.5
Signal shape of $D^+ \rightarrow \tau^+\nu_\tau$	1.1
Total systematic uncertainty	9.9

respectively. This is the first measurement of the branching fraction of $D^+ \rightarrow \tau^+\nu_\tau$ to date. With $\mathcal{B}_{\mu\nu} = (3.74 \pm 0.17) \times 10^{-4}$ [1], we find $R_{\tau/\mu} = 3.21 \pm 0.64_{\text{stat.}} \pm 0.43_{\text{syst.}}$, which is consistent with the standard model prediction of 2.67. From Eq. (1), with the inputs shown in Table III and assuming $|V_{cd}| = 0.22438 \pm 0.00044$ from the global fit [1], we obtain

$$f_{D^+} = 224.5 \pm 22.8_{\text{stat.}} \pm 11.3_{\text{syst.}} \pm 0.9_{\text{ext-syst.}} \text{ MeV},$$

where the last uncertainty is due to external input parameters. This is consistent with the average between the recent four-flavor LQCD predictions of Refs. [22, 23], $f_{D^+} = 212.6 \pm 0.6$ MeV, as well as with the experimental results for $D^+ \rightarrow \mu^+\nu_\mu$ from the BESIII [2] and the CLEO [3] Collaborations.

TABLE III. External input parameters with uncertainties from Ref. [1].

Parameter	Value
m_μ	$0.1056583745(24)$ GeV
m_τ	$1.77686(12)$ GeV
M_{D^+}	$1.86965(5)$ GeV
τ_{D^+}	$1.040(7)$ ps
G_F	$1.1663787(6) \times 10^{-5}$ GeV $^{-2}$

Taking the average prediction for f_{D^+} from [22] and [23], we find

$$|V_{cd}| = 0.237 \pm 0.024_{\text{stat.}} \pm 0.012_{\text{syst.}} \pm 0.001_{\text{ex-syst.}}$$

This is consistent with both the world average $|V_{cd}| = 0.218 \pm 0.004$ [1] and the global fit result [1].

The BESIII collaboration thanks the staff of BEPCII and the IHEP computing center for their strong support. This work is supported in part by National

Key Basic Research Program of China under Contract No. 2015CB856700; National Natural Science Foundation of China (NSFC) under Contracts No. 11625523, No. 11635010, and No. 11735014; National Natural Science Foundation of China (NSFC) under Contract No. 11835012; the Chinese Academy of Sciences (CAS) Large-Scale Scientific Facility Program; Joint Large-Scale Scientific Facility Funds of the NSFC and CAS under Contracts No. U1532257, No. U1532258, No. U1732263, and No. U1832207; CAS Key Research Program of Frontier Sciences under Contracts No. QYZDJ-SSW-SLH003 and No. QYZDJ-SSW-SLH040; 100 Talents Program of CAS; INPAC and Shanghai Key Laboratory for Particle Physics and Cosmology; German Research Foundation DFG under Contract No. Collaborative Research Center CRC 1044, FOR 2359; Istituto Nazionale di Fisica Nucleare, Italy; Koninklijke Nederlandse Akademie van Wetenschappen (KNAW) under Contract No. 530-4CDP03; Ministry of Development of Turkey under Contract No. DPT2006K-120470; National Science and Technology fund; The Knut and Alice Wallenberg Foundation (Sweden) under Contract No. 2016.0157; The Royal Society, UK under Contract No. DH160214; The Swedish Research Council; U.S. Department of Energy under Contracts No. DE-FG02-05ER41374, No. DE-SC-0010118, and No. DE-SC-0012069; and University of Groningen (RuG) and the Helmholtzzentrum für Schwerionenforschung GmbH (GSI), Darmstadt.

-
- [1] M. Tanabashi *et al.* (Particle Data Group), *Phys. Rev. D* **98**, 030001 (2018).
 - [2] M. Ablikim *et al.* (BESIII Collaboration), *Phys. Rev. D* **89**, 051104(R) (2014).
 - [3] B. I. Eisenstein *et al.* (CLEO Collaboration), *Phys. Rev. D* **78**, 052003 (2008).
 - [4] B. A. Dobrescu and A. S. Kronfeld, *Phys. Rev. Lett.* **100**, 241802 (2008).
 - [5] S. Bifani *et al.*, *J. Phys. G* **46**, 023001 (2019); J. P. Lees *et al.* (BABAR Collaboration), *Phys. Rev. Lett.* **109**, 101802 (2012); M. Huschle *et al.* (Belle Collaboration), *Phys. Rev. D* **92**, 072014 (2015); R. Aaij *et al.* (LHCb Collaboration), *Phys. Rev. Lett.* **115**, 111803 (2015); Y. Sato *et al.* (Belle Collaboration), *Phys. Rev. D* **94**, 072007 (2016); S. Hirose *et al.* (Belle Collaboration), *Phys. Rev. Lett.* **118**, 211801 (2017); R. Aaij *et al.* (LHCb Collaboration), *Phys. Rev. Lett.* **120**, 171802 (2018); **113**, 151601 (2014); *J. High Energy Phys.* **08** (2017) 055.
 - [6] A. G. Akeroyd and C. H. Chen, *Phys. Rev. D* **75**, 075004 (2007).
 - [7] C. H. Yu *et al.*, *Proceedings of IPAC 2016, Busan, Korea, 2016*.
 - [8] M. Ablikim *et al.* (BESIII Collaboration), *Chin. Phys. C* **37**, 123001 (2013); *Phys. Lett. B* **753**, 629 (2016).
 - [9] M. Ablikim *et al.* (BESIII Collaboration), *Nucl. Instrum.*

- Methods Phys. Res., Sect. A **614**, 345 (2010).
- [10] S. Jadach, B. F. L. Ward and Z. Was, *Phys. Rev. D* **63**, 113009 (2001).
 - [11] E. Barberio and Z. Was, *Comput. Phys. Commun.* **79**, 291 (1994).
 - [12] D. J. Lange, *Nucl. Instrum. Methods Phys. Res., Sect. A* **462**, 152 (2001); R. G. Ping, *Chin. Phys. C* **32**, 599 (2008).
 - [13] K. Nakamura *et al.* (Particle Data Group), *J. Phy. G* **37**, 075021 (2010) and 2011 partial update for the 2012 edition.
 - [14] J. C. Chen, G. S. Huang, X. R. Qi, D. H. Zhang, and Y. S. Zhu,, *Phys. Rev. D* **62**, 034003 (2000); Y. Rui-Ling *et al.*, *Chin. Phys. Lett.* **31**, 061301 (2014).
 - [15] S. Agostinelli *et al.*, *Nucl. Instrum. Methods Phys. Res., Sect. A* **506**, 250 (2003); J. Allison *et al.*, *IEEE Trans. Nucl. Sci.* **53**, 270 (2006); Z. Y. Deng *et al.*, *High Energy Phys. Nucl. Phys.* **30**, 371 (2006).
 - [16] R. M. Baltrusaitis *et al.* (MARK III Collaboration), *Phys. Rev. Lett.* **56**, 2140 (1986); J. Adler *et al.* (MARK III Collaboration), *Phys. Rev. Lett.* **60**, 89 (1988).
 - [17] M. Ablikim *et al.* (BESIII Collaboration), *Phys. Rev. D* **97**, 072004 (2018).
 - [18] M. Ablikim *et al.* (BESIII Collaboration), *Chin. Phys. C* **42**, 083001 (2018).
 - [19] H. Albrecht *et al.* (ARGUS Collaboration), *Phys. Lett. B* **241**, 278 (1990).
 - [20] M. Ablikim *et al.* (BESIII Collaboration), *Phys. Rev. D* **94**, 032001 (2016).
 - [21] K. S. Cranmer, *Comput. Phys. Commun.* **136**, 198 (2001).
 - [22] N. Carrasco *et al.* (ETM Collaboration), *Phys. Rev. D* **91**, 054507 (2015).
 - [23] A. Bazavov, C. Bernard, N. Brown, C. DeTar, A. X. El-Khadra *et al.* (Fermilab Lattice and MILC Collaborations), *Phys. Rev. D* **98**, 074512 (2018).